Journal of the Chilean Chemical Society
ISSN 0717-9707 *versión on-line*

J. Chil. Chem. Soc. v.50 n.3 Concepción sep. 2005

J. Chil. Chem. Soc., 50, N° 3 (2005), págs: 617-623

Magnetic properties of spinel-type oxides $NiMn_{2-x}Me_xO_4$

O. PEÑA[1,*], C. MOURE[2], V. BODENEZ[1], X. CAILLEAUX[1], B. PIRIOU[1], J. ORTIZ[3,&], G.ZÚÑIGA[3], J.L.GAUTIER[3,&],P.N. LISBOA-FILHO[4]

1. *Chimie du Solide et Inorganique Moléculaire, UMR 6511. CNRS - Université de Rennes 1. Institut de Chimie de Rennes, 35042 Rennes cedex, FRANCE*
2. *Instituto de Cerámica y Vidrio, CSIC. Campus de Cantoblanco, 28049 Madrid. SPAIN*
3. *LEFQS Dpto. de Química de Materiales. Facultad de Química y Biología. Universidad de Santiago. 7254758 Santiago. CHILE*
4. *Departamento de Física, Universidade Estadual Paulista (UNESP), 17033-360, Bauru SP. BRAZIL*

ABSTRACT

New materials, based on the well-known spinel compound $NiMn_2O_4$, have been synthesized and characterized from the magnetic point of view. The manganese cation was partially substituted in the general formula $NiMn_{2-x}Me_xO_4$, by nonmagnetic and magnetic elements, such as *Me* = Ga, Zn, Ni and Cr (0 x 1). Prior to the determination of their magnetic properties, the non-substituted spinel $NiMn_2O_4$ was carefully characterized and studied as a function of the oxygen stoichiometry, based on the influence of the annealing atmosphere and quenching rate. The ferrimagnetic character was observed in all samples, with a paramagnetic-to-ferromagnetic transition temperature T_c stabilized at 110 K, and well defined long-range antiferromagnetic interactions at lower temperatures, which depend on the applied field and the substitute concentration.

Keywords : magnetic oxides, spinels, magnetic exchange, ferrimagnetic properties

---

INTRODUCTION

Spinel materials based on 3-d transition-metal oxides of Mn and Ni, have been well studied due to their outstanding semiconducting properties. Their fields of application concern mainly temperature sensing devices, as for instance, the negative temperature coefficient (NTC) thermistors [1-3]. For this reason, a thorough research has been developed, focused mainly on varying cation compositions, chemical phase relations, structural and electrical properties, etc. [4-6]. But, in contrast to other related compounds based mainly on Fe [7], almost none of these reports have dealt with the magnetic properties, in particular those occurring at low temperature [8]. Because of the relative complexity of the cationic distribution, any research in these materials must take into account the intrinsic duality among the tetrahedral and octahedral sites, and the possibility of the cations to adopt two, or even three, different oxidation states within the same specimen. In addition, a good knowledge of the energy level distribution is of primary importance to properly describe the molecular orbitals which participate to the basic magnetic properties in the paramagnetic as well as in the ordered state(s).

It becomes then interesting to study such compounds from the point of view of their electrical and magnetic aspects in order to establish any eventual correlation which may lead to potential applications, such as in the recently investigated giant-magnetoresistance ferromagnetic perovkites. During the recent years,

we have developed a research centered on the crystallo-chemical and physical properties of manganite compounds of spinel structure. In a first stage, we have been looking into the magnetic properties of the parent compound $NiMn_2O_4$, already well described in the literature [9-12], in order to characterize the influence of the partial oxygen pressure during annealing and the modification of the magnetic properties with the oxygen stoichiometry. In a second step, the manganese cation has been partially substituted by other transition metal elements, in particular nonmagnetic ones in order to separate out the contribution of the main magnetic sublattice. In a third step, the cobalt cation has been incorporated into the structure, fully modifying the magnetic response of the spinel material [13,14]. We report herein the synthesis, the structural characterization and the magnetic behavior of pseudo-binary oxides of spinel structure, of general formula $NiMn_{2-x}Me_xO_4$, where *Me* can be a transition metal as well as non-transition elements, such as Cu, Zn, Cr, Mg, Ga, etc, including Ni (to form the binary oxide Ni_2MnO_4, when x(*Me*) = 1.0).

EXPERIMENTAL

Samples were prepared using different methods, based mainly on solid-state mixing of the corresponding oxides, or using hydrated nitrates as precursors. The parent compound $NiMn_2O_4$ was prepared in every case, thus allowing a direct comparison of the different techniques of synthesis used in this work. Absolutely no difference was detected from the crystallographic and magnetic points of view.

In the case of samples prepared by a direct mixing of oxides of submicronic particle size, the stoichiometric mixtures were homogenized by wet attrition milling using isopropanol as liquid medium. The mixtures were calcined at 900 C for several hours. The materials were milled again, uniaxially pressed and sintered at 1050 C for 2 h, with a heating rate of 5 C/min and cooling in air at a rate of 2 C/min. When using nitrates, the corresponding mixtures were first warmed up during 36 hours at 150 C in order to evaporate the water molecules. The obtained gel-like product was then heated at 450 C overnight and finally calcined at 900 C for 12 hours. The sintering process was finally carried out at 1100 C for 2 hours, with similar warming and cooling speeds as described above.

The series $NiMn_{2-x}Cr_xO_4$ was prepared by a technique of thermal decomposition of nitrates. For this, nickel, chromium and manganese nitrates, dissolved in water at 1 $mol.dm^{-3}$ were mixed in stoichiometric quantities, to prepare compositions for x = 0.0, 0.25, 0.5, 0.75 and 1.0; these quantities were checked by atomic absorption in a plasma of argon. The aqueous solutions were dried at 90 C until full decomposition of nitrates, leaving pure oxides as remaining products. After mechanical attrition, the corresponding powders were calcined at 800 C for 48 hours and furnace-cooled down to room temperature. Final attrition and sieving were performed prior to X-ray diffraction analyses. In order to properly describe the influence of the oxygen partial pressure, the as-prepared non-substituted compound $NiMn_2O_4$ was treated under different temperatures, gas flow atmospheres (air, argon and O_2) and cooling rates. A full description of the X-ray diffraction (XRD) results, scanning electron microscope (SEM) observations, elemental analysis using energy dispersion spectrometry (EDX) and X-ray photoelectron spectroscopy (XPS), can be found in reference [15]. Results are just recalled herein for completeness and further comparison.

Chemical formulas given all throughout the text correspond to nominal starting concentrations. The metal-to-metal ratio 1:2 ($Ni:Mn_{2-x}Me_x$) was verified by energy dispersive X-ray spectroscopy (EDX) and in all cases confirmed the nominal metallic composition, within an experimental error of 5-8 %. Based on our results obtained in the non-substituted system $NiMn_2O_{4-d}$ (ref. 15, and summarized here below, §.3.2.1), which indicated an oxygen content varying between $O_{3.774}$ and $O_{4.230}$ depending on the oxygen partial pressure during annealing, all samples were calcined under conditions of normal air pressure. With this procedure, an oxygen stoichiometry of 3.913.98 was obtained, as systematically determined by wet chemical methods, either through iodometric titration [16] or by using $VOSO_4$ as a soft reducing agent [12].

X-ray diffraction (XRD) patterns were recorded at the final step of synthesis on an INEL diffractometer using CuKa radiation and Si as an internal standard. The microstructure was observed with a scanning electron microscope (Jeol, JSM 6301F). Magnetic measurements were performed in a SHE VTS-906 and a Quantum Design MPMS XL5 SQUID susceptometers, between 2 K and 300 K, on ceramic specimens glued to a thin rod in order to avoid disorientation due to torque forces exerted on the sample. When samples were only available in powder form, compact pellets were prepared to avoid any orientation of fine cristallites under the applied field. Additional characterization by a.c.

techniques was performed using a homemade mutual-inductance susceptometer.

RESULTS AND DISCUSSION

Crystallochemical characterization

Figure 1 shows XRD patterns for typical samples of spinel structure, in particular samples of the solid solution resulting from the substitution of manganese by nickel [$NiMn_2O_4Ni_2MnO_4$] and the partial substitution of Mn by Zn in $NiMn_{2-x}Zn_xO_4$ (x = 0.25 and 0.5). In all cases, the XRD patterns could be indexed in the classical spinel space group *Fd3m* of cubic symmetry, with no visible impurities within the experimental detection limit. Samples purity was confirmed by SEM-EDX analyses, which showed a homogeneous resulting product, with particles of typical dimensions of 3 mm, uniformly distributed on the surface (figure 2). All details concerning EDX analyses and lattice parameter variations are given elsewhere [17,18].

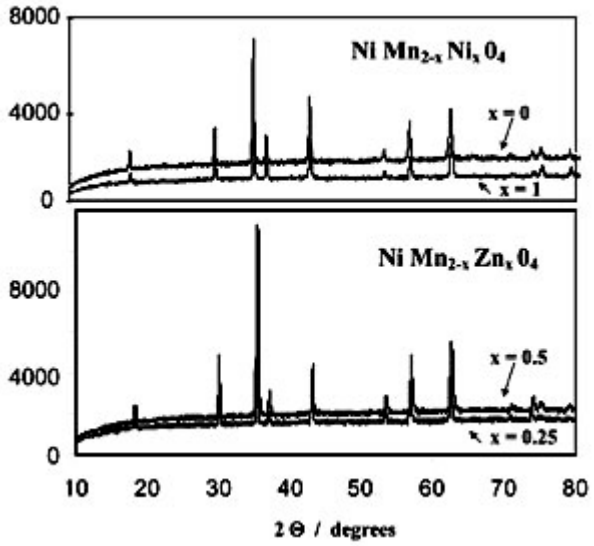

Figure 1. X-ray diffraction patterns (intensity in arbitrary units) of $NiMn_2O_4$ and Ni_2MnO_4(top panel); $NiMn_{1.75}Zn_{0.25}O_4$ and $NiMn_{1.5}Zn_{0.5}O_4$(bottom panel)

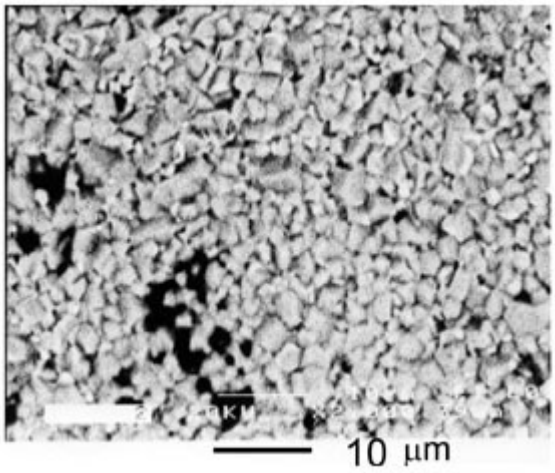

Figure 2. Scanning electron microscopy image (SEM) of a sample of nominal composition $Ni_{1.25}Mn_{1.75}O_4$

Magnetic properties

The parent compound $NiMn_2O_4$

As in most of the magnetically-ordered oxide systems, the thermal variation of the magnetization greatly depends on the applied field. In addition, the oxygen stoichiometry, which can be monitored through the oxygen partial pressure and the quenching conditions, can modify the magnetic response of these materials [15]. In order to fix the experimental conditions, we first of all performed the magnetic characterization of the non-substituted spinel $NiMn_2O_4$, under various conditions of preparation and applied field. Figure 3 shows the magnetic response of a $NiMn_2O_4$ sample annealed at 1100 C and quenched in air, and measured on a ZFC/FC mode under an applied d.c. field of 5 Oe. For this, the sample was first cooled under zero field (ZFC), the measuring field was applied, and the sample was then heated at a slow rate (~ 1 K/min) while recording its magnetization; on the FC mode, the sample was cooled at a similar rate, under the same applied field. In this figure, two well-defined anomalies can be observed: during the ZFC mode, a first broad maximum occurs at about 45 K followed by an antiferromagnetic-type transition at T_N = 101 K. The paramagnetic state is reached at T_c = 105 K. During the field cooling (FC) procedure, the magnetization increases abruptly at the magnetic transition temperature T_c, while the low temperature anomaly is seen as a leveling of the magnetization variation. Such double-transition feature (confirmed by a.c. susceptibility measurements; not shown) have been already observed [8,19] and it is a signature of a complex magnetic structure which reflects the competition between ferromagnetic (F) and antiferromagnetic (AF) sublattices leading to a ferrimagnetic-like state.

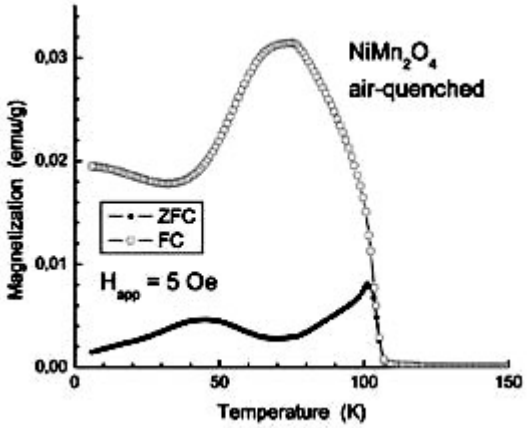

Figure 3. ZFC/FC cycle measured under 5 Oe, for a $NiMn_2O_4$ sample annealed at 1100 C and quenched in air

In a second stage, we measured the same sample under different applied fields. Figure 4 shows the M(T) variation measured from 5 K up to room temperature, under magnetic fields of 250 and 1000 Oe. It is immediately seen that T_c stays unchanged at 105 K, independent of the applied field. In the ordered state, the two transitions which were observed at low fields merge into a single broad transition, which gets broader and takes place at lower temperatures when applying larger fields. This maximum, which occurs at T_{max}, defines the antiferromagnetic-like ordering, typical of non-compensated ferromagnetic systems (either ferrimagnetic sublattices or canted antiferromagnetism). Obviously, at low applied fields (i.e., a.c. measurements), T_{max} corresponds to the characteristic temperature T_N defined in figure 3.

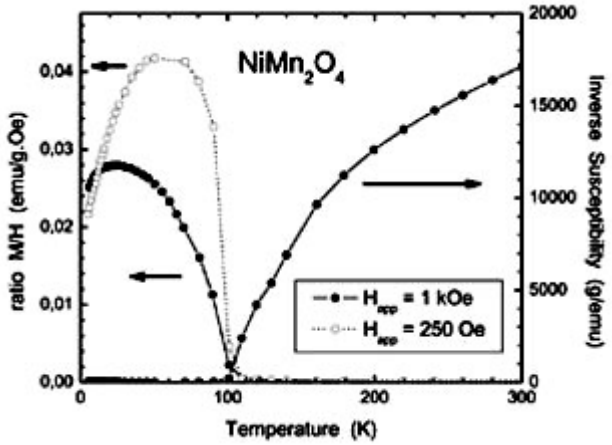

Figure 4. Thermal variation of the magnetization (left) and the inverse susceptibility (right) for the non substituted compound $NiMn_2O_4$

presents a negative curvature due to a temperature-independent paramagnetic term c_{TIP} or because the experimental conditions approach the magnetic ordering (fig. 4). The effective moment was calculated in the range [200K-300K], where c^{-1} varies almost linearly with temperature yielding a value of 6.62 ± 0.02 m_B, which corresponds to 4.3 m_B per Mn ion, supposing that Ni stays in its 2+ oxidation state with an effective moment of 2.83 m_B (Table I). This value may suggest a mixed state between Mn^{3+} and Mn^{4+}, although titration analysis performed on a similar sample [15] gave an analytical formula of $Ni_{0.92}Mn^{3+}_{1.980}Mn^{4+}_{0.012}O_{3.914}$, that is manganese is almost fully 3+ ; this difference on the expected ratio Mn^{3+}/Mn^{4+} probably comes from subtle modifications in the oxygen stoichiometry in the $NiMn_2O_{4-d}$ system. The Curie-Weiss temperature 0 is negative, of the order of -86 K, indicating that strong antiferromagnetic interactions exist in this compound, besides the ferromagnetic character which sets at T_c. As a consequence, $NiMn_2O_4$ can be considered as a ferrimagnetic compound, as expected in most of the spinel materials.

Table I. Magnetic data [(a)] for the series $NiMn_{2-x}Me_xO_4$ (*Me* = Ga, Zn, Cr, Ni)

	Weiss Temp. Θ (K) (± 5 K)	magnetic moment μ_{eff} (μ_B/f.u.) [(b)] (± 0.05)
$NiMn_2O_4$	-86	6.62
$NiMn_{1.75}Ga_{0.25}O_4$	-208	6.75
$NiMn_{1.50}Ga_{0.50}O_4$	-275	7.27
$NiMn_{1.75}Zn_{0.25}O_4$	-250	6.82
$NiMn_{1.50}Zn_{0.50}O_4$	-265	7.45
$NiMn_{1.75}Cr_{0.25}O_4$	-168	6.55
$NiMn_{1.50}Cr_{0.50}O_4$	-195	6.57
$NiMn_{1.25}Cr_{0.75}O_4$	-235	6.58
$NiMn_{1.00}Cr_{1.00}O_4$	-267	6.60
$Ni_{1.25}Mn_{1.75}O_4$	-139	6.27
$Ni_{1.50}Mn_{1.50}O_4$	-183	6.15
$Ni_{1.75}Mn_{1.25}O_4$	-214	6.18
$Ni_{2.00}Mn_{1.00}O_4$	-245	6.10

(a) magnetic data calculated in the experimental range [200K T 300K]

(b) magnetic moment per formula unit

From now on, all other experimental data shown in this work have been taken under an applied field of 1 k. The reason for this is twofold: such a field gives a reasonable good signal for even very small samples (down to 10-mg samples) and, on the other hand, the magnetic phenomena observed at low temperature are still sharply defined.

Partial substitution in $NiMn_{2x}Me_xO_4$ by nonmagnetic elements (Me = Ga, Zn)

Nonmagnetic metals like gallium and zinc were partially substituted for manganese in order to modify and eventually weaken the long-range magnetic interactions. Two nominal compositions were retained for this analysis : x = 0.25 and 0.5. The paramagnetic-ferromagnetic transition at T_c decreases very slightly, from 105 K down to approximately 90 K (figures 5 and 6). The antiferromagnetic interactions look more affected, since the Weiss parameter 0 largely increases, while the effective moment almost does not change in absolute values at low doping (x = 0.25), although it increases if normalized to the Mn concentration. This trend is confirmed at higher substitution, since the effective moment reaches 7.3 -7.4 m_B per formula unit (Table I). This net increase of the magnetic moment must be associated to a re-ordering of the magnetic cations in the tetrahedral and octahedral sites. This phenomenon is a classical demonstration of the cationic redistribution in the spinel structure. Indeed, when replacing Zn^{2+} for iron in the mixed ferrites for example, Fe^{3+} ions move towards the octahedral sites since Zn^{2+} occupies preferentially the tetrahedral positions [20]. As a result, the net magnetization M_A of the tetrahedral sublattice decreases, while the magnetization M_B of the octahedral sublattice stays almost constant. Then, the total magnetization M_T ($M_T = M_B-M_A$), of antiferromagnetic origin, increases when the nonmagnetic ion replaces the magnetic one. This model applies quite well to our solid solution $NiMn_{2-x}Zn_2O_4$ if we consider the cationic distribution proposed in ref. 21 for the non substituted compound, $(Ni_{1-v}Mn_v)[Ni_vMn_{2-v}]O_4$, where the parentheses designate the tetrahedral A-sites, and the brackets, the octahedral B-sites, and *v* denotes de degree of inversion [22].

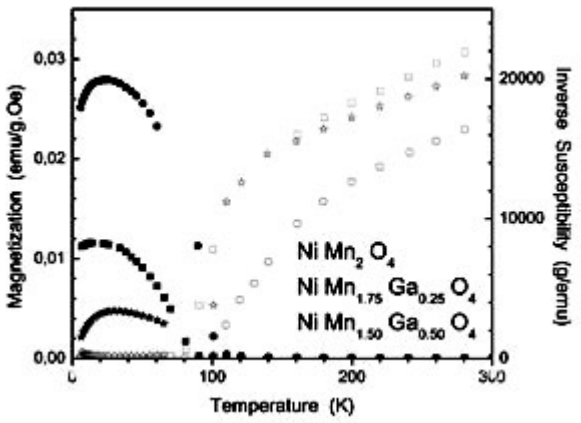

Figure 5. Thermal variation of the magnetization (left, filled symbols) and the

inverse susceptibility (right, empty symbols) for $NiMn_2O_4$ (circles), $NiMn_{1.75}Ga_{0.25}O_4$ (squares) and $NiMn_{1.50}Ga_{0.50}O_4$ (stars)

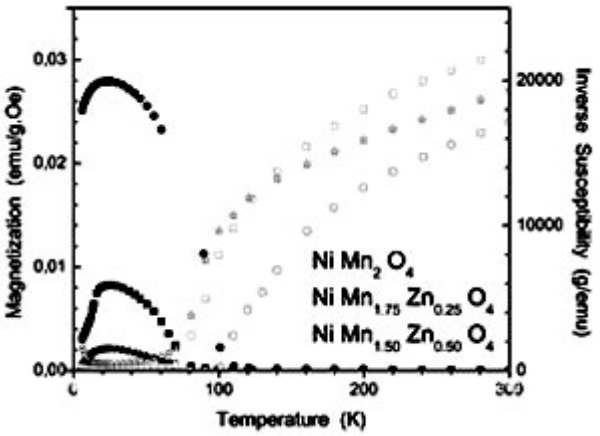

Figure 6. Thermal variation of the magnetization (left, solid symbols) and the inverse susceptibility (right, open symbols) for $NiMn_2O_4$ (circles), $NiMn_{1.75}Zn_{0.25}O_4$ (squares) and $NiMn_{1.50}Zn_{0.50}O_4$ (stars)

Partial substitution in $NiMn_{2x}Me_xO_4$ by magnetic elements (Me = Cr, Ni ; 0.0 £ x £ 1.0)

Once the effect of magnetic dilution has been well established, we proceeded with the effects of substitution of magnetic transition-metal elements, like nickel and chromium. Figures 7.a and 7.b show the thermal variation of the magnetic moment and the inverse susceptibility for the whole series $NiMn_{2x}Cr_xO_4$, measured under 1 k. Figure 8 shows the paramagnetic region of the inverse susceptibility for the series $NiMn_{2x}Ni_xO_4$ (that is, $Ni_{1+x}Mn_{2-x}O_4$). Again, the paramagnetic-to-ferromagnetic transition at T_c does not change with the substitution, staying at 105-110 K for all samples described in this section. The characteristic temperature T_{max}, defining the long-range antiferromagnetic order stays constant. However, there is a net increase of the Weiss parameter 0, which measures the strength of the antiferromagnetic interactions (Table I).

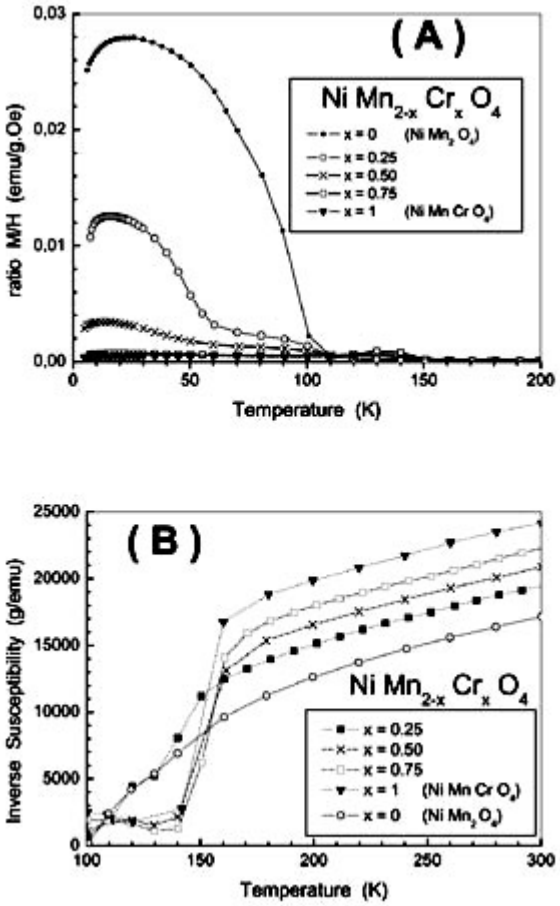

Figure 7. Thermal variation of the magnetization (A) and the inverse susceptibility (B) for the solid solution $NiMn_{2-x}Cr_xO_4$

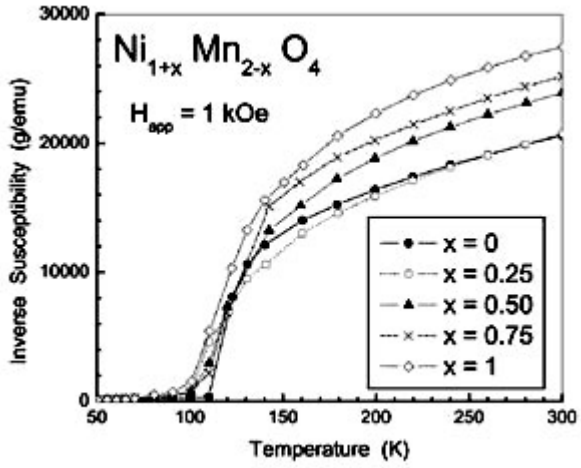

Figure 8. Inverse susceptibility for the solid solution $NiMn_{2-x}Ni_xO_4$

Figure 9 shows this steady increase of 0 (in negative values) with x(Cr) and x(Ni). However, the evolution of the effective moment m_{eff} follows different trends in the case of nickel compared to chromium. In the case

that Cr^{3+} would be substituting Mn^{4+} or, Cr^{2+} substituting Mn^{3+}, since they have the same magnetic moment in their high-spin state. On the other hand, the effective moment of the solid solution $NiMn_{2x}Ni_xO_4$ decreases when x(Ni) increases; this variation is due to the substitution of Mn ions by Ni^{2+}, hence by a magnetic ion having a lower magnetic moment.

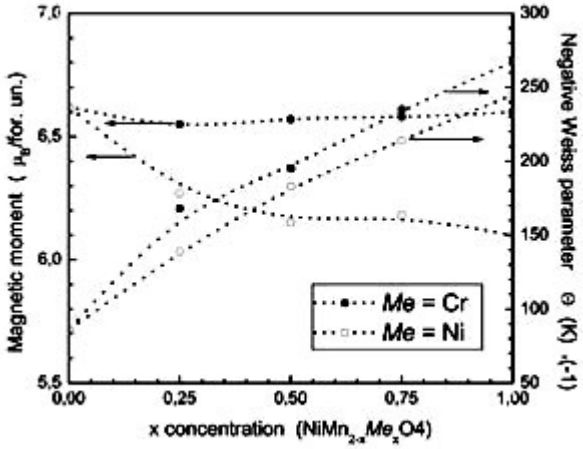

Figure 9. Evolution of the magnetic moment m_{eff} (left axis) and the negative Weiss parameter Q (right axis) for the solid solutions $NiMn_{2-x}Cr_xO_4$ (solid symbols) and $NiMn_{2-x}Ni_xO_4$ (open symbols)

CONCLUSIONS

We have prepared and characterized several solid solutions based on the wellknown spinel compound $NiMn_2O_4$, in which the manganese ion was partially substituted by non-magnetic (Ga and Zn) and magnetic (Cr and Ni) elements. The actual insertion of the substituent into the spinel structure was successful, as confirmed by XRD data and SEM observations. Prior to the magnetic characterization, a thorough study of the annealing conditions (oxygen pressure, temperature, time and quenching rates) for the non-substituted compound was necessary, in order to interpret the magnetic results and fix the best reproducible conditions for the rest of the work.

In all cases, the paramagnetic-to-ferrimagnetic transition temperature stayed constant or with a very slight variation. However, the Curie-Weiss temperature 0 increased enormously, reaching values of the order of the experimental conditions (e.g., -250 K or more). The magnetic moment, calculated per unit formula showed different variations, depending on the oxidation state of the substituent. Thus, presence of Ni^{2+} transforms part of the Mn^{3+} ions into Mn^{4+}, of lower magnetic moment, while the substitution of Mn by Cr left the effective moment unchanged, meaning that Cr^{2+} was probably substituting Mn^{3+}. For the non-magnetic substitutions, a rearrangement of the cations must be considered, since large ions (like Zn^{2+}) make the Mn ions to move from the tetrahedral towards the octahedral sites, producing an

unbalance of the net magnetization due to the sum of both sublattices. All these examples demonstrate the enormous versatility of the spinel structure to host different elements with varying oxidation states, producing a wide range of magnetic phenomena.

ACKNOWLEDGEMENTS

Authors from Chile and O.P. thank projects Fondecyt-Chile 1020066, 7020066 and 1050178. Authors from France and Brazil thank project CAPES/COFECUB 416/03. Authors from France thank Région Bretagne for financial support.

REFERENCES

[1] N.W. Grimes. Phys. Technol., **6**, 22-27 (1975)

[2] J.L. Martin de Vidales, P. Garcia-Chain, R.M. Rojas, E. Vila, O. Garcia-Martinez. J. Mater. Science, **33**, 1491-1496 (1998)

[3] R. Schmidt, A. Stiegelschmitt, A. Roosen, A.W. Brinkman. J. Eur. Ceram. Soc., **23**, 1549-1558 (2003)

[4] Y. Abe, T. Meguro, S. Oyamatsu, T. Yokoyama, K. Komeya. J. Mater. Science, **34**, 4639-4644 (1999)

[5] S. Baliga, A.L. Jain. Mater. Lett., **11**, 226-228 (1991)

[6] T. Yokoyama, Y. Abe, T. Meguro, K. Komeya, K. Kondo, S. Kaneko, T. Sasamoto. Jpn. J. Appl. Phys., **35**, 5775-5780 (1996)

[7] T.A.S. Ferreira, J.C. Waerenborgh, M.H.R.M. Mendonça, M.R. Nunes, F.M. Costa. Solid State Sciences **5**, 383-392 (2003)

[8] C. Boudaya, L. Laroussi, E. Dhahri, J.C. Joubert, A. Cheikh-Rouhou. Phase Transitions, **68**, 631-642 (1999)

[9] T. Hashemi, A.W. Brinkman. J. Mater. Res., **7**, 1278-1282 (1992)

[10] C. Drouet, C. Laberty, J.L.G. Fierro, P. Alphonse, A. Rousset. J. Inorg. Mater., **2**, 419-426 (2000)

[11] Xiao-Xia Tang, ,A. Manthiram, J.B. Goodenough. J. Less-Common Metals, **156**, 357-368 (1989)

[12] J. Ponce, E. Ríos, J.L. Rehspringer, G. Poillerat, P. Chartier, J.L. Gautier. J.Solid State Chem., **145**, 23-32 (1999)

[13] Yanwei Ma, M. Bahout, O. Peña, P. Duran, C. Moure. Bol. Soc. Esp. Ceram. V., **43**, 663-667 (2004)

[14] O. Peña, Yanwei Ma, M. Bahout, P. Duran, C. Moure, M.N. Baibich,

G. Martinez. phys. stat. sol. **(c), 1**, S31-S34 (2004)

[15] P.N. Lisboa-Filho, M. Bahout, P. Barahona, C. Moure, O. Peña. J. Phys. Chem. Solids, **66**, 1206-1212 (2005)

[16] P. Barahona, V. Bodenez, T. Guizouarn, O. Peña, J. Ortiz, E. Ríos, R. Pastene, J.L. Gautier. J. Chil. Chem. Soc., **50**, 495-499 (2005)

[17] V. Bodenez. DEA report, Université de Rennes 1, june 2003

[18] X. Cailleaux, B. Piriou. Internal report, Magistere Matériaux, Université de Rennes 1, june 2003

[19] Y. Shen, T. Nakayama, M. Arai, O. Yanagisawa, M. Izumi. J. Phys. Chem. Solids, **63**, 947-950 (2002)

[20] A. Herpin, Théorie du Magnétisme, Presses Universitaires de France, Paris, (1968), pp 654-656

[21] B. Boucher, R. Buhl, M. Perrin. Acta Cryst. **B25**, 2326-2333 (1969)

[22] K.E. Sickafus, J.M. Wills, N.W. Grimes. J. Am. Ceram. Soc., **82**, 3279-3292 (1999)
